Journal Pre-proof

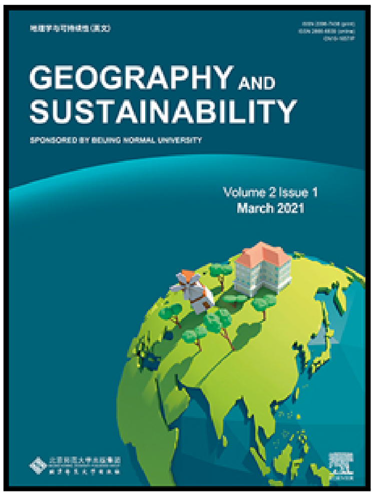

Wind farms increase land surface temperature and reduce vegetation productivity in the Inner Mongolia Plateau

Luyao Liu , Pengtao Liu , Jiawei Yu , Gang Feng , Qing Zhang ,
Jens-Christian Svenning

PII: S2666-6839(24)00007-5
DOI: https://doi.org/10.1016/j.geosus.2024.01.007
Reference: GEOSUS 175

To appear in: *Geography and Sustainability*

Received date: 7 August 2023
Revised date: 28 January 2024
Accepted date: 29 January 2024

Please cite this article as: Luyao Liu , Pengtao Liu , Jiawei Yu , Gang Feng , Qing Zhang , Jens-Christian Svenning , Wind farms increase land surface temperature and reduce vegetation productivity in the Inner Mongolia Plateau, *Geography and Sustainability* (2024), doi: https://doi.org/10.1016/j.geosus.2024.01.007

Highlights

- The wind farms in the Inner Mongolia are clustered in geographical patterns.
- Wind farms slightly affect daytime LST but significantly warm nighttime LST.
- Wind farms reduce the vegetation’s net primary productivity.

Research Article

Wind farms increase land surface temperature and reduce vegetation productivity in the Inner Mongolia Plateau

Luyao Liu[a,b,c], Pengtao Liu[a,d], Jiawei Yu[a], Gang Feng[a], Qing Zhang[a,e,*],Jens-Christian Svenning[f,g]

[a]Ministry of Education Key Laboratory of Ecology and Resource Use of the Mongolian Plateau, School of Ecology and Environment, Inner Mongolia University, Hohhot 010021, China
[b]CAS Key Laboratory of Forest Ecology and Management, Institute of Applied Ecology, Chinese Academy of Sciences, Shenyang 110016, China
[c]College of Resources and Environment, University of Chinese Academy of Sciences, Beijing 100049, China
[d]Inner Mongolia Autonomous Region Ecological and Agricultural Meteorological Centre, Hohhot, 010051, China
[e]Collaborative Innovation Center for Grassland Ecological Security (Jointly Supported by the Ministry of Education of China and Inner Mongolia Autonomous Region), Hohhot 010021, China
[f]Center for Ecological Dynamics in a Novel Biosphere (ECONOVO), Department of Biology, Aarhus University, Ny Munkegade 114, DK-8000 Aarhus C, Denmark
[g]Center for Biodiversity Dynamics in a Changing World (BIOCHANGE), Department of Biology, Aarhus University, Ny Munkegade 114, DK-8000 Aarhus C, Denmark

*__Corresponding author:__ Qing Zhang.
E-mail addresses: liuluyao789@163.com (Luyao Liu), birdlpt@163.com (Pengtao Liu), yjiawei959@163.com (Jiawei Yu), qaufenggang@163.com (Gang Feng), qzhang82@163.com (Qing Zhang), svenning@bio.au.dk (Jens-Christian Svenning).

Graphical Abstract

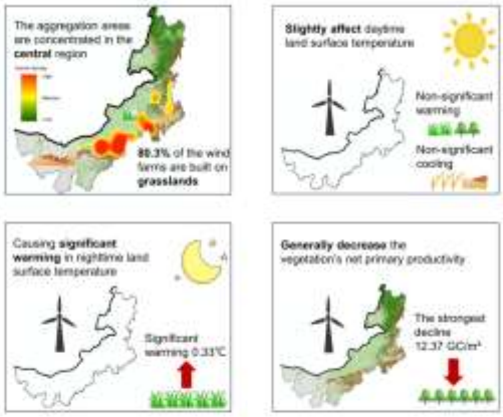

Abstract

Wind power has been developing rapidly as a key measure to mitigate human-driven global warming. The understanding of the development and impacts of wind farms on local climate and vegetation is of great importance for their rational use but is still limited. In this study, we combined remote sensing and on-site investigations to identify wind farm locations in Inner Mongolia and performed landscape pattern analyses using Fragstats. We explored the impacts of wind farms on land surface temperature (LST) and vegetation net primary productivity (NPP) between 1990 and 2020 by contrasting these metrics in wind farms with those in non-wind farm areas. The results showed that the area of wind farms increased rapidly since 1990 to 10,755 km^2 by 2020. Spatially, wind farms are mainly clustered in three aggregation areas in the center. Further, wind farms increased nighttime LST, with a mean value of 0.23 °C, but had minor impacts on the daytime LST. Moreover, wind farms caused a decline in NPP, especially over forest areas, with an average reduction of 12.37 GC/m^2. Given the impact of wind farms on LST and NPP, we suggest that the development of wind farms should fully consider their direct and potential impacts. This study provides scientific guidance on the spatial pattern of future wind farms.

Keywords: *Wind farm, Landscape pattern, LST, NPP, Inner Mongolia Plateau*

1. Introduction

Global warming is a severe challenge for humanity, and global temperature is expected to increase by 1.5 °C in the next two decades (Steffen et al., 2018; Kemp et al., 2022). Greenhouse gas emissions are the cause of global warming (Lashof and Ahuja, 1990). Promoting clean energy is crucial to reducing greenhouse gas emissions (Haines et al., 2007). James Bryce built the first wind farm (WF) in Scotland in 1887 (Leung and Yang, 2012). As low-carbon clean energy, wind power shows great potential and plays an important role in global power systems (Xia and Song, 2009; Howland et al., 2019). By 2020, wind power has grown to account for more than 6% of global power (C2ES, 2020). In 2021, the installed capacity of global wind power increased by 93.6 GW, and the total installed capacity reached 837 GW (Council, 2022). With the rapid development of wind power, the ecological and environmental problems caused by wind farms an issue of increasing importance (Sawant et al., 2021).

Understanding the changing landscape pattern of wind farm area use is fundamental for the reasonable development of wind power. Previous research has been conducted on the national scale (Ayodele et al., 2018), provincial scale (Moradi et al., 2020), and regional scale (Van Haaren and Fthenakis, 2011). The top three countries with wind farm installed capacity are China, the United States, and Germany (S. Zhang et al., 2020). Wind farms often occupy different land cover types, such as cropland, forest, grassland, and desert (Deng et al., 2011; Xu et al., 2019; X. Zhang et al., 2020). Wind farms usually heterogenous landscape placement, associated with wind energy potential (Xia and Song, 2009) as well as factors such as environmental justice (Avila, 2018) and social capital (Van der Horst and Toke, 2010). In recent years, landscape indices have been used to assess the fragmentation and connectivity of wind farms (Diffendorfer et al., 2019; Guo et al., 2020).

With the large number of wind farms, the impacts of wind farms on the local climate have received more and more attention (Sawant et al., 2021). Previous studies have often assessed the impacts of wind farms on local climate based on field observations or model simulations (Keith et al., 2004; Moradi et al., 2020). In recent years, MODIS data has been widely used to evaluate land surface temperature (LST) due to its wide spatial coverage, high resolution, and good spatial-temporal continuity (Harris et al., 2014). Some studies used MODIS data to evaluate the impacts of wind farms on LST in the United States (Zhou et al., 2012; Qin et al., 2022). LST of daytime and nighttime are two commonly used indices (Zhou et al., 2012). Many studies have found that wind farms can cause an increase in nighttime LST (Zhou et al., 2012; Xia et al., 2016). However, the impacts of wind farms on daytime LST are controversial. Some studies have confirmed that wind farms have no significant effect on daytime LST (Slawsky et al., 2015). Some studies have shown that wind farms can increase daytime LST (Moravec et al., 2018). The impacts of wind farms on LST vary in different geographic regions. Wind farms lead to a decline in winter nighttime LST in Europe but a rise in winter nighttime LST in North America (Keith et al., 2004). Compared with the Americas and Europe, research about the impacts of wind farms on LST in Asia is rare (Chang et al., 2016; Luo et al., 2021). Therefore, exploring the impacts of wind farms on LST in Asia is necessary.

The impact of wind farms on vegetation net primary productivity (NPP) is also a hot issue (Saidur et al., 2011; Leung and Yang, 2012). Field surveys and remote sensing simulation are two commonly used methods. The former is usually used for local wind farms (Fagúndez, 2009), while the latter is often used for large-scale regional wind farms (Qin et al., 2022). The impacts of wind farms on NPP are controversial. Some studies showed an inhibitory effect of wind farms on NPP (Y. Liu et al., 2021). Some studies proposed that wind farms can promote vegetation growth and increase NPP (Li et al., 2018; Xu et al., 2019). Other studies found no significant effects of wind farms on NPP (Xia and Zhou, 2017; Luo et al., 2021). Importantly, a variety of other potential impacts of wind farms need to be considered in area planning and to receive more research attention, e.g., impacts on biodiversity such as birds (Drewitt and Langston, 2006; Fox et al., 2006) and fish (Bergström et al., 2013), as well as on ecosystem functions and services, e.g., cultural services (Sibille et al., 2009), as well as on human health (Hurtado et al., 2004).

As an important part of the Eurasian steppe, the Inner Mongolia Plateau is rich in wind resources and flat, suitable for wind farm construction (Zeng et al., 2014). In 1989, the first wind farm was completed in this area. By 2021, the wind farms installed capacity are 39.93 million kilowatts, ranking first in China (Bureau, 2022). Although the research on wind farms in this region has received extensive attention, most of them focus on wind energy assessment of wind farms (Wu et al., 2013), power generation optimization of wind farms (Dong et al., 2013), and carbon emissions of wind farms (P. Liu et al., 2021). However, there are no reports about the impacts of wind farms on local climate and vegetation. Therefore, this study extracted the locations of wind farms from 1990 to 2020 in the Inner Mongolia Plateau to answer three key questions: What are the changing trends in the landscape pattern of wind farm area use in the Inner Mongolia Plateau? What are the impacts of wind farms on local LST and NPP?

This study first provides an overview of the development and construction of wind farms in Inner Mongolia, followed by a further exploration of the impact of wind farms on LST and NPP. It consists of five sections. Section 2 describes the process of extracting wind farm locations and analyzing landscape patterns and introduces the research methods for exploring the impact of wind farms on LST and NPP. The landscape pattern changes of the wind farms and their effects on the ecological environment are presented in section 3. Sections 4 and 5 provide discussions and conclusions, respectively.

2. Materials and methods

2.1. Overview of the study area

Inner Mongolia is equal to the Inner Mongolia Autonomous Region of the administrative region (37°30′ N–53°20′ N, 97°10′ W–126°02′ W), located in the north of China. The terrain is dominated by high plains, with an altitude of 600–2000 m. It has a temperate continental climate with rich wind resources. The Inner Mongolia Plateau is one of the regions with the most abundant wind energy resources in China, with an average annual wind speed of 4–6 m/s (Institute of Geographic Sciences and Natural Resources Research, 2007). Mean annual precipitation ranges from 40–500 mm, increasing from southwest to northeast. The mean annual temperature ranges from -4.6 °C to 9.1 °C (P. Liu et al., 2021). The land cover type is mainly grassland, in addition to forest, cropland, and others (Fig. 1). Inner Mongolia Plateau is an important energy base in China, not only rich in coal, oil, and natural gas but also rich in cleaner energy resources such as wind and solar energy (Zeng et al., 2014). The Inner Mongolia Plateau is rich and unique in biodiversity. As a representative of grassland culture, Inner Mongolia also has importance to the ecological civilization goal for China (Q. Zhang et al., 2020).

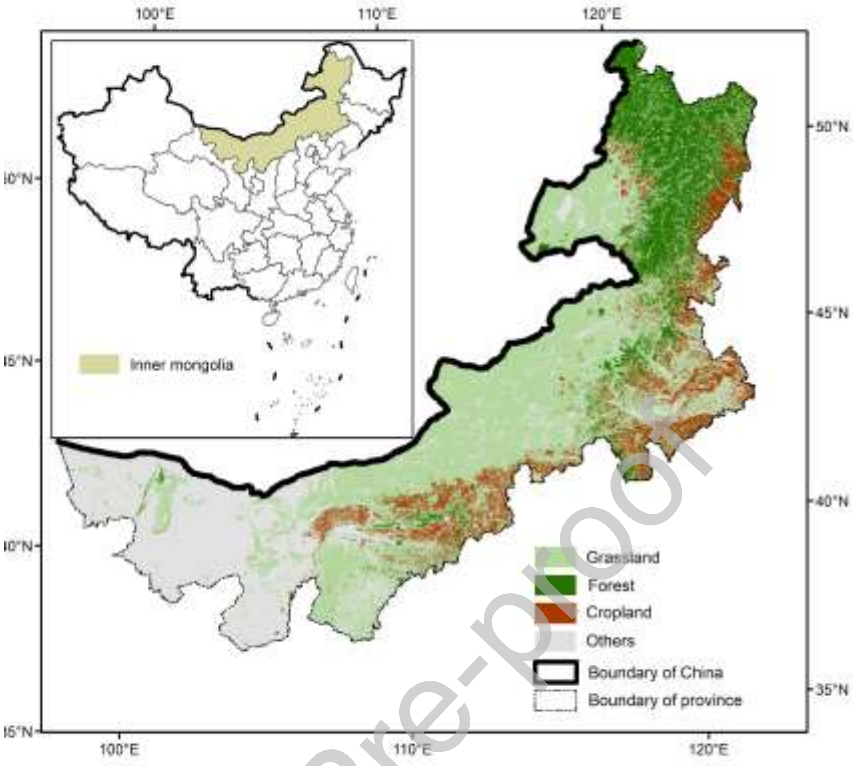

Fig. 1. Overview of the study area. (a) The geographical location of Inner Mongolia in China; (b) Land cover types in Inner Mongolia include grasslands, forested areas, cultivated lands, and other varieties.

2.2. Development trend of wind farms in Inner Mongolia

To further understand the development trend of wind farms in Inner Mongolia, we collected data on the electricity generation from the main modes in Inner Mongolia from 1990 to 2020 (such as thermal power, hydropower, wind farms, and photovoltaic power generation) and the installed capacity of wind farms. We then calculated the proportion of each mode in the total electricity generation over the years to examine the changing trend of wind farms. The data was sourced from the Inner Mongolia Energy Statistical Yearbook (http://tj.nmg.gov.cn/) and the China Electric Power Statistical Yearbook (https://www.yearbookchina.com/).

2.3. Wind farm location extraction

The visual interpretation method is applied in the extraction of wind farm location information. The remote sensing data mainly included Landsat TM, ETM+, OLI data (http://www.gscloud.cn/, http://landsat.usgs.gov), and Gaofen-1 (GF-1) PMS data (http:// www.cresda.com/CN/). Before visual interpretation, geometric correction, image fusion, and enhancement were performed on remote sensing data. The detailed visual interpretation methodology is outlined in Supplemental file. Using this approach, we extracted the location data for wind farms constructed in Inner Mongolia between 1990 and 2020, as well as for all existing wind farms. These findings have undergone and passed accuracy validation.

2.4. Land cover types of wind farms

To reveal the land cover type of wind farm constructed in the Inner Mongolia plateau, we overlaid land cover data and wind farm boundary data using ArcGIS10.2. The land cover data were obtained from the Institute of Geographical Sciences and Resources of the Chinese Academy of Sciences (http://www.geodata.cn/) for the period 1990–2020 with a spatial resolution of 30 m. Land cover types were classified into four categories: forest, grassland, cropland, and others (Fig. 1). Other land types mainly include unutilized land types, such as saline-alkali land, sandy land, and bare soil.

2.5. Landscape pattern analysis of wind farms

We selected the number of patches, area mean, Euclidean mean nearest neighbor distance, and patch cohesion index to assess the landscape pattern change of wind farms from 1990 to 2020. Mean nearest neighbor distance and patch cohesion index represents the degree of spatial clustering (Schumaker, 1996; Su et al., 2022). The landscape indices were calculated using Fragstats 4.2.

2.6. Spatial distribution characteristics of wind farms

In order to estimate the spatial distribution of wind farms, we first use kernel density estimation to determine the spatial distribution density map of wind farms (Bonnier et al., 2019). Then, the Mean Centre tool in the ArcGIS software is used to locate the region's geographic center of gravity of wind farms. In order to further reveal the distribution direction and dispersion degree of the gravity center area of wind farms, the standard deviation ellipse tool was performed. The long half-axis of the ellipse represents the distribution direction of wind farms, and the short half-axis represents the distribution dispersion degree of wind farms. The longer the short half-axis, the greater the distribution dispersion degree (Yuan et al., 2020).

2.7. Impacts of wind farms on surface temperature

To reveal the impacts of wind farms on local climate, we compared the difference in LST between wind farms and non-wind farms. Previous studies have shown that wind farms directly impact the surrounding environment at 0–2 km, while this impact is ignored at more than 4 km (Harris et al., 2014). Thus, the buffer zone above 4 km is generally considered a control area (Chang et al., 2016; Tang et al., 2017). In this study, the buffer zone 4–6 km away from the wind farms is defined as a non-wind farm (Fig. 2(a), Fig. 2(b)). To eliminate differences between wind farms and non-wind farms in microclimate due to the differences in topography, we used a 5-year time window (Harris et al., 2014; Qin et al., 2022). The construction year is centered on a two-year forward and backward extension. For example, the evaluation years for wind farms built in 2010 are 2008–2012 (Fig. 2(c)). The resulting LST difference is only attributed to the impacts of wind farms (Fig. 2(c)). The value of wind farms impacts on LST is the difference between the change in LST in the wind farm ($\Delta \mathrm{LST}_{\mathrm{WF}}$) and the non-wind farm ($\Delta \mathrm{LST}_{\mathrm{NWF}}$). The equation for the impacts of wind farms on LST can be expressed as follows:

$$\Delta \mathrm{LST} = \Delta \mathrm{LST}_{\mathrm{WF}} - \Delta \mathrm{LST}_{\mathrm{NWF}} = \mathrm{LST}_{\mathrm{Trend}_{\mathrm{WF}}} \times \Delta T - \mathrm{LST}_{\mathrm{Trend}_{\mathrm{NWF}}} \times \Delta T \quad (1)$$

where $\mathrm{LST}_{\mathrm{Trend}_{\mathrm{WF}}}$ and $\mathrm{LST}_{\mathrm{Trend}_{\mathrm{NWF}}}$ represent the LST linear fit trends of wind farms and non-wind farms, expressed in units of °C/year. ΔT represents the 5-year time window. The data from MODIS LST data (https://developers.google.com/earth-engine/datasets/catalog/MODIS_061_MOD11A1). Terra and Aqua are the two common climate satellites. Terra data are available from 2000, two years ahead of Aqua, so we chose Terra satellite data for the calculation. The spatial resolution of Terra is 1 km, and the temporal resolution is one day. Because LST data are currently available from 2000–2020, the available wind farms data are from 2002–2018 under the restricted 5-year window, and data for other years are excluded. In this study, the LST is divided into daytime and nighttime two indicators to evaluate and further evaluate the impacts of wind farms on LST in different seasons, spring (March-May), summer (June-August), autumn (September to November), and winter (December to February).

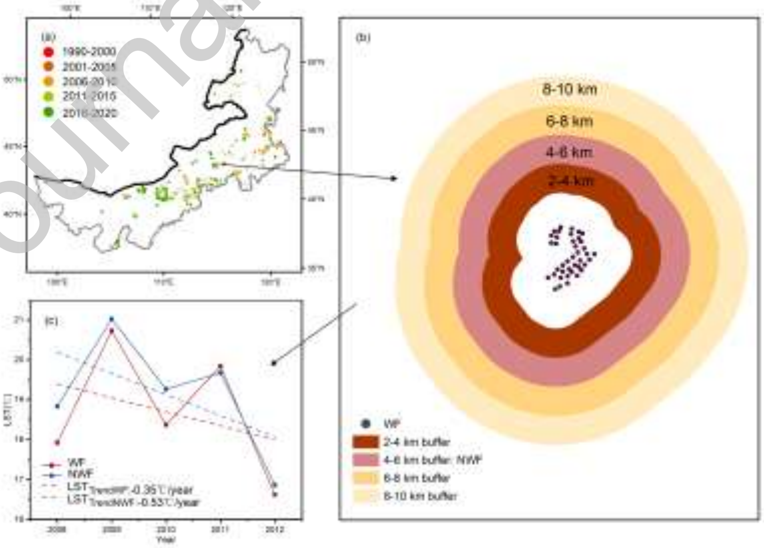

Fig. 2. Schematic diagram of the impacts of wind farms on LST. *Note*: (a) shows the locations of wind farms constructed in Inner Mongolia over the years. (b) for comparison, a wind farm (WF) patch and its buffer zone define a 4–6 km buffer zone as a non-wind farm (NWF) area. (c) The example wind farm was constructed in 2010, and the wind farm was linearly fitted with the LST of non-wind farms from 2008–2012. The red represents wind farm, $\mathrm{LST}_{\mathrm{Trend}_{\mathrm{WF}}}$ is

-0.35 °C/year, so it the $\Delta \mathrm{LST_{WF}}$ is -1.74 °C under the 5-year time window; blue represents non-wind farm, $\mathrm{LST_{Trend_{NWF}}}$ is -0.53 °C/year, $\Delta \mathrm{LST_{NWF}}$ is -2.64 °C in the 5-year time window, that is, the temperature of the wind farm is 0.9 °C higher than that of the non-wind farm in 5 years.

2.8. Impacts of wind farms on local vegetation

In addition, to reveal the impacts of wind farms on NPP, we also quantified the wind farm compared with the non-wind farm (Tang et al., 2017). NPP data from MODIS (https://e4ftl01.cr.usgs.gov/MOLT/MOD17A3HGF.006/). The spatial resolution is 500m, and the time range used is 2000–2018. The equation for the impacts of wind farms on NPP can be expressed as follows:

$$\Delta \mathrm{NPP} = \Delta \mathrm{NPP_{WF}} - \Delta \mathrm{NPP_{NWF}} = \mathrm{NPP_{Trend_{WF}}} \times \Delta T - \mathrm{NPP_{Trend_{NWF}}} \times \Delta T \quad (2)$$

where $\mathrm{NPP_{Trend_{WF}}}$ and $\mathrm{NPP_{Trend_{NWF}}}$ represent the linearly fitted trends of NPP for wind farms and non-wind farms, multiplied by ΔT (time window) to obtain the change values at the 5-year time, which are $\Delta \mathrm{NPP_{WF}}$ and $\Delta \mathrm{NPP_{NWF}}$, respectively.

3.Results

3.1. Evolution of wind power from 1990 to 2020

The power generation mode in Inner Mongolia has developed from a single-generation structure to the current pattern of multiple-generation modes. From 1990 to 2006, the power generation was almost entirely thermal power (Fig. 3(a)). The proportion of wind power generation has increased rapidly since 2006 and accounted for 14.12% of total electricity generation by 2020 (Fig. 3(b)). Over the past three decades, the installed capacity of wind farms has grown from 1.765×10^4 kilowatts in 1990 to 3.785×10^7 kilowatts in 2020, an increase of >2000 times (Fig. 3(c)). Wind power generation increased from 0.14 billion kWh in 1990 to 82.05 billion kWh in 2020, an increase of nearly 6000 times (Fig. 3(d)).

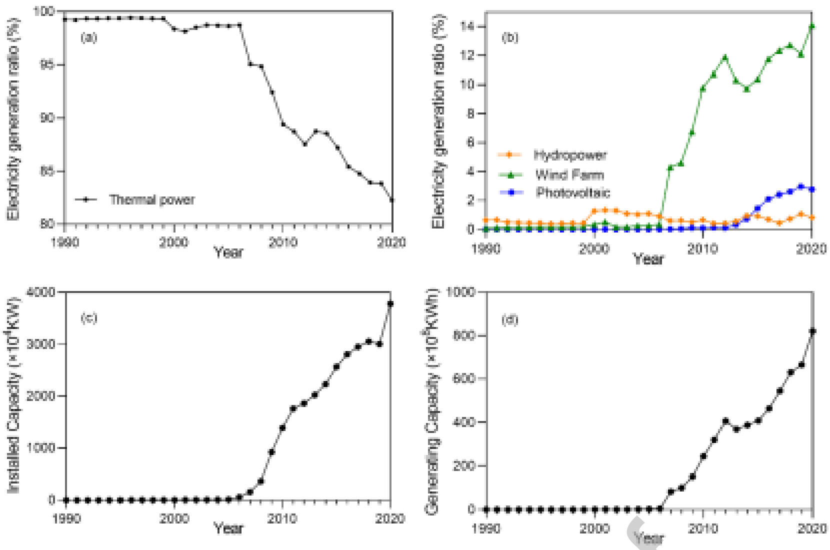

Fig. 3. Electricity generation in the Inner Mongolia from 1990 to 2020. (a) Ratio of electricity generation of thermal power; (b) Ratio of power generation of clean energy; (c) Wind farms installed capacity; (d) Wind power generation capacity.

3.2. Landscape pattern change of wind farms from 1990 to 2020

From 1990 to 2020, the construction area of wind farms in the Inner Mongolia increased from 1.2 km^2 to 10,755.0 km^2 (Fig. 4(a)). Of the land occupied by wind farms, 80.3% is grassland, 10.6% is cropland, and the rest is forest and other land cover types (Fig. 4(b)). The number of patches continued to increase to 226 by 2020 (Fig. 4(c)). The area mean showed a trend of rapid increase, then showed a slow decrease and then show increase, reaching a maximum of 5,600.90 km^2 in 2009 (Fig. 4(d)). The mean nearest neighbor decreased year by year to 14,366 m in 2020 (Fig. 4(e)). The patch cohesion index showed an increasing trend, reaching 94.60 by 2020 (Fig. 4(f)). Wind farms exhibit three aggregation areas, one in the east and two in the central part of the Inner Mongolia Plateau (Fig. 5(a)). The gravity center area of wind farms shows a "northeast-southwest" distribution pattern (Fig. 5(c)). The long-half axis and short-half axis of the standard deviation ellipse are increased during the 30 years, indicating gradually expanding scope and increasing dispersion degree.

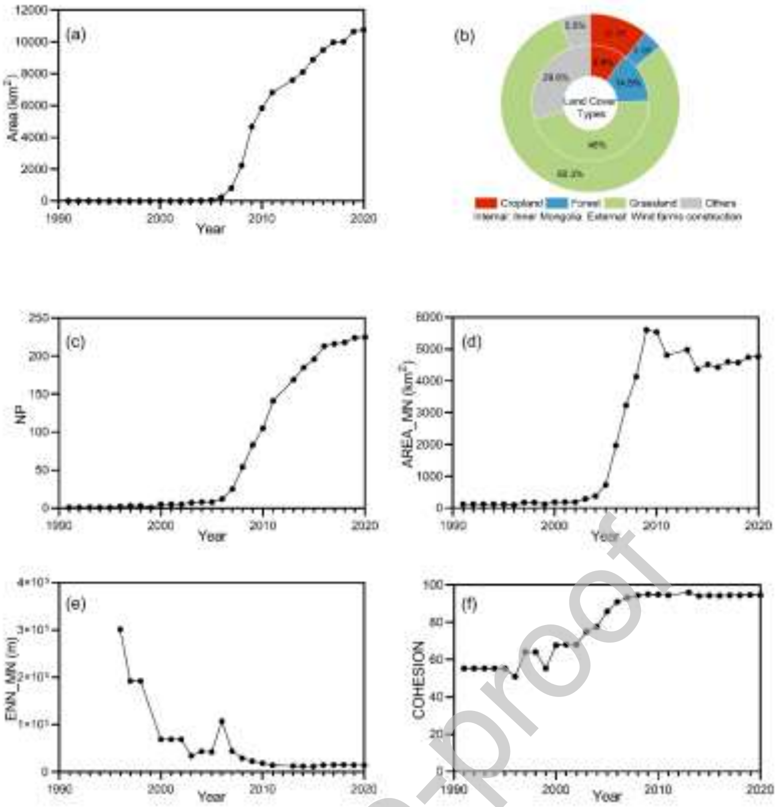

Fig. 4. Landscape index of wind farms in the Inner Mongolia. (a) Annual wind farm construction area (Area); (b) The internal refers to the proportion of land cover types in Inner Mongolia, while the external represents the proportion of land cover types occupied by wind farms; (c) Number of wind farm patches (NP); (d) Mean patch area of wind farms (AREA_MN); (e) The mean geometric nearest neighbor distance (ENN_MN) among wind farms; (f) Cohesion index (COHESION) of wind farms.

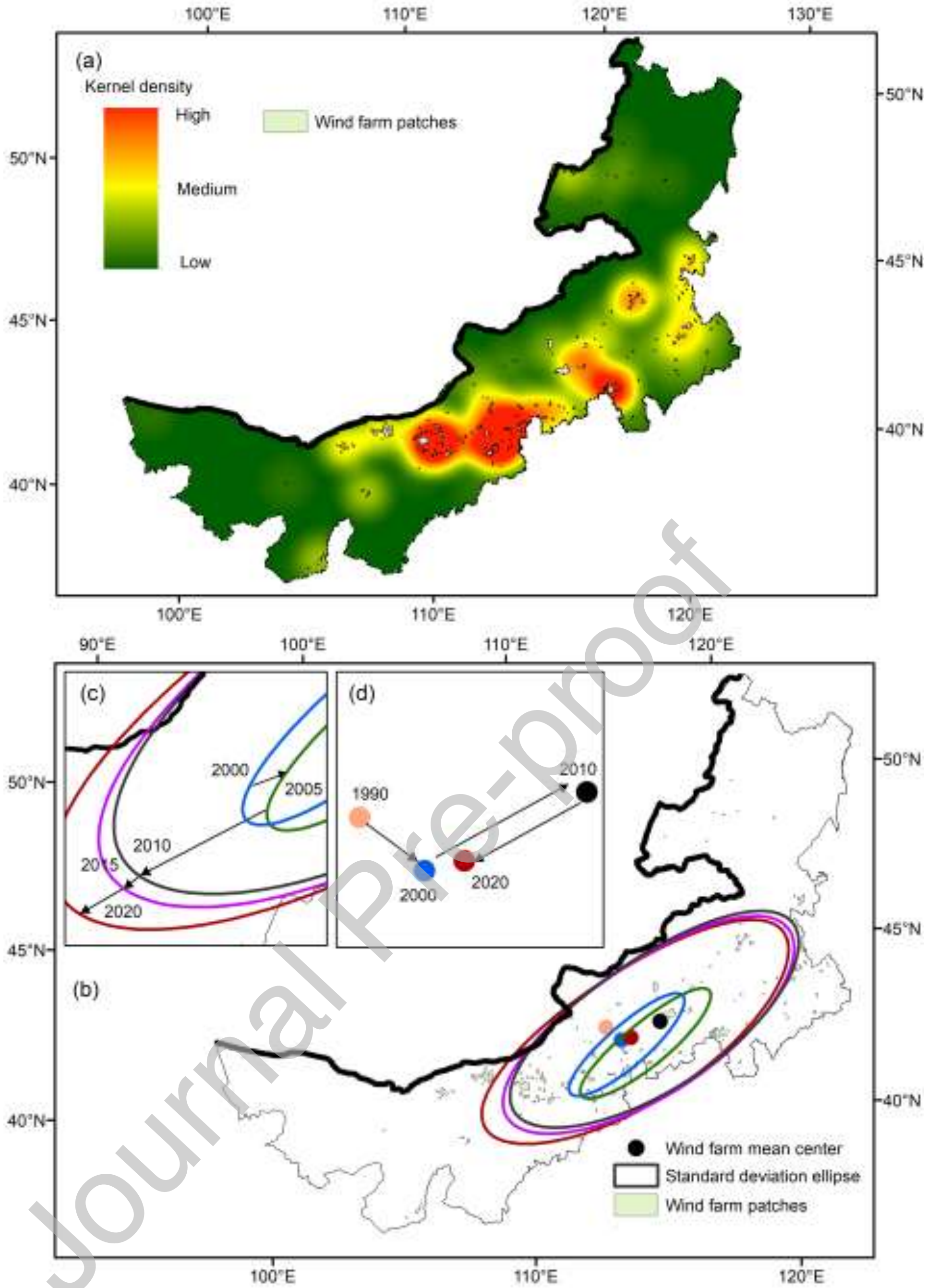

Fig. 5. Spatial distribution characteristics of wind farms in the Inner Mongolia. *Note*: (a) was a kernel density analysis of wind farms. Red represents the high patch density of wind farms; Green represents the low density. (b) provides an overview of wind farms' gravity center and standard deviation ellipse. (c) represents standard deviation ellipses of wind farms for 2000, 2005, 2010, 2015, and 2020, respectively. And the direction of their time series movement. (d) represents the gravity centers of 1990, 2000, 2010, and 2020 with round dots, respectively. The arrows indicate the moving direction.

3.3. Impacts of wind farms on surface temperature

The impacts of wind farms on daytime and nighttime LST in the Inner Mongolia

Plateau are very different. The daytime LST affected by wind farms showed non-significant warming (p>0.05), with an average ΔLST of 0.14 ± 2.34 °C. Among them, the number of warming and cooling wind farms accounted for 56% and 44% of all wind farms, respectively (Fig. 6(a), Fig. 6(b)). Wind farms built on different land cover types did not affect daytime LST. Although grassland (0.20 ± 2.42) and forest (0.08 ± 1.56) tended to exhibit warming effects and viceversa for cropland (-0.04 ± 2.32) and other land covers (-0.12 ± 1.84), none of them were significant (p>0.05; Fig. 6(c)). Similarly, wind farms had minor impacts on daytime LST in spring (-0.004 ± 0.48, p>0.05), summer (0.02 ± 0.37, p>0.05), autumn (-0.002 ± 0.47, p>0.05), or winter (0.04 ± 0.05, p>0.05) (Fig. 6(d)).

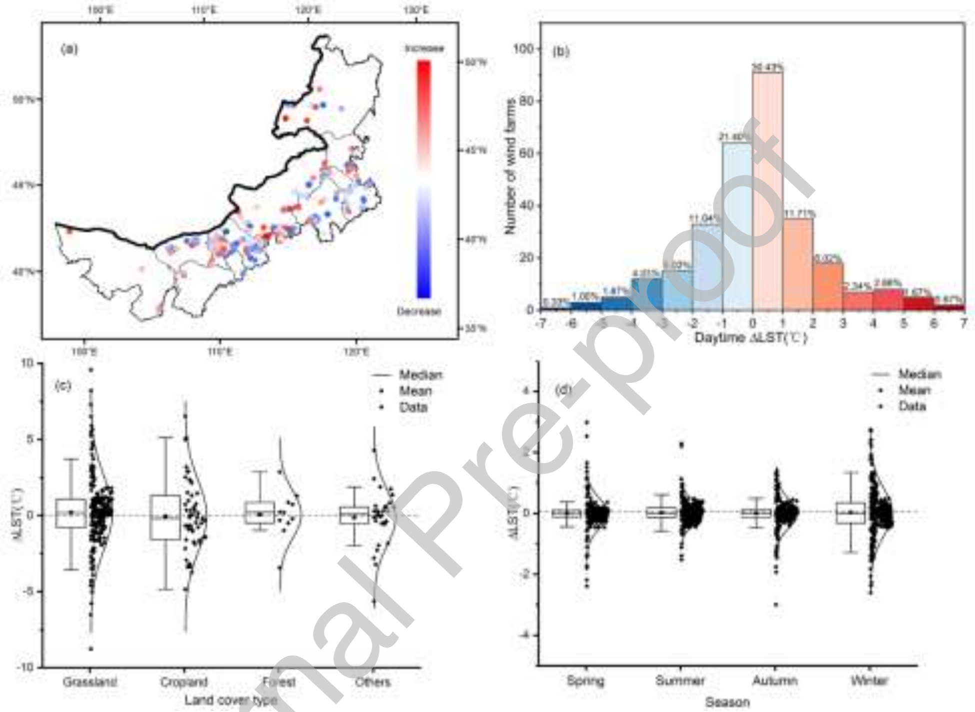

Fig. 6. Impacts of wind farms on daytime LST. (a) illustrates the spatial distribution of the warming (indicated in red) and cooling (indicated in blue) effects attributed to wind farms. (b) presents a histogram distribution of daytime ΔLST, with the horizontal axis signifying the magnitude of LST changes and the vertical axis representing the number of wind farms. (c) shows the daytime ΔLST across different land cover types. Meanwhile, (d) shows the daytime ΔLST across different seasons.

Wind farms had a significant warming impact on nighttime LST (p<0.05) with an average ΔLST of 0.23 ± 1.62 °C. The proportion of wind farms exhibiting warming or cooling effect was 56% and 44%, respectively (Fig. 7(a), Fig. 7(b)). The extent of the impacts of wind farms on nighttime LST varied among land cover types. Specifically, grassland (0.33 ± 1.50, p<0.05) exhibited a significant warming effect, while there were minor effects in the forest (0.19 ± 1.32, p>0.05), other land covers (0.24 ± 2.56, p>0.05), and cropland (-0.13 ± 1.47, p>0.05) (Fig. 7(c)). The impacts of wind farms on nighttime LST also varied among different seasons, with significant warming in summer (0.02 ± 0.11, p<0.05) and autumn

(0.09 ± 0.42, $p<0.01$), but minor effect in spring (0.007±0.23, $p>0.05$) and winter (-0.01±0.54, $p>0.05$) (Fig. 7(d)).

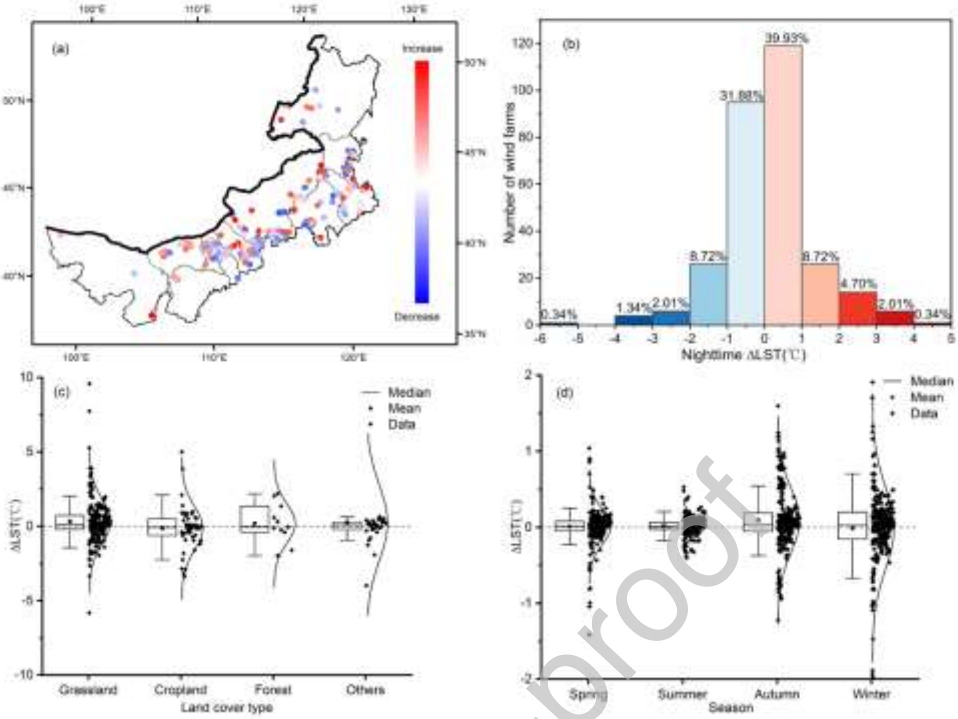

Fig. 7. Impacts of wind farms on nighttime LST. (a) illustrates the spatial distribution of the warming (indicated in red) and cooling (indicated in blue) effects attributed to wind farms. (b) presents a histogram distribution of nighttime ΔLST, with the horizontal axis signifying the magnitude of LST changes and the vertical axis representing the number of wind farms. (c) shows the nighttime ΔLST across different land cover types. Meanwhile, (d) shows the nighttime ΔLST across different seasons.

3.4. Impacts of wind farms on vegetation productivity

Compared with the NPP in non-wind farm buffer areas, the NPP in wind farms showed a significant decrease (-5.04 ± 23.97 GC/m^2, $p<0.01$). 53% of wind farms exhibited reduced NPP, and 47% of wind farms elevated NPP (Fig. 8(a), Fig. 8(b)). The wind farm effect on NPP differed across land cover types. The NPP of the forest was most affected by wind farms (-12.37 ± 22.22 GC/m^2), with grassland ranking second (-4.48 ± 25.03 GC/m^2), and just minor effects in other land covers (-4.10 ± 13.39 GC/m^2) and cropland (-3.77 ± 17.26 GC/m ^{2}) (Fig. 8(c)).

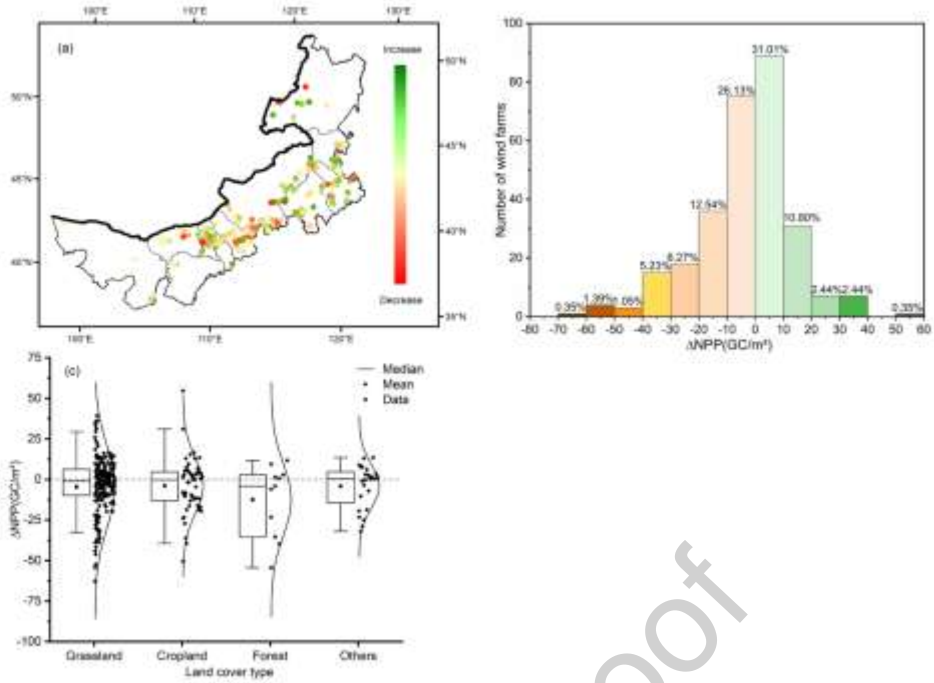

Fig. 8. Impacts of wind farms on NPP. (a) illustrates the spatial distribution of the decreasing (indicated in red) and increasing (indicated in blue) effects attributed to wind farms. (b) presents a histogram distribution of NPP, with the horizontal axis signifying the magnitude of NPP changes and the vertical axis representing the number of wind farms. (c) shows the ΔNPP across different land cover types.

4. Discussion

Wind power has become an essential part of new energy development in the Inner Mongolia Plateau in recent years (Zeng et al., 2014), with wind power development having gone through three stages: slow exploration, rapid expansion, and stable development (Dai et al., 2018). As a vital wind power base in China, Inner Mongolia accounts for 40% of the available wind energy in the country (Zeng et al., 2014). Since the release of the renewable energy policy in 2006, wind farms have expanded rapidly. During the ten years from 2006 to 2015 in the Inner Mongolia Plateau, the annual average patch growth number, annual average growth area, annual average installed capacity, and annual average power generation of wind farms was 18.5 (Fig. 4(c)), 866.42km^2 (Fig. 4(a)), 250.66 million kilowatts (Fig. 3(c)), and 40.29 billion kilowatt hours (Fig. 3(d)), respectively. The growth of the above indicators was 30.83 times, 154.85 times, 198.24 times, and 176.70 times, respectively. Thus, it can be seen that national policies have driven the development of wind power (T. Liu et al., 2022).

The Inner Mongolia Plateau's flat terrain and low population density are advantageous for wind farm construction in the region (Wu et al., 2013). This study found that the gravity center of wind farms moved in a "northeast-southwest" direction (Fig. 5(c)), consistent with the center of the national economic development. In the early stage of wind farm construction, the Inner Mongolia Plateau adopted a large number of centralized wind power construction models (Zeng et al., 2014). Because of the rapid economic development of North China and Beijing city, these regions showed great demand for electricity. With the national policy of western development, the economy in the western region has developed rapidly, and the electricity demand has increased. Meanwhile, China began exploring decentralized wind power development mode in 2011 (Dai and Xue, 2015). The distribution of wind farms further expanded (Fig. 5(b)), and the gravity center moved to the southwest (Fig. 5(c)). By 2020, wind farms were clustered, forming three aggregation areas in the Inner Mongolia Plateau (Fig. 5(a)).

This study found that wind farms had a minor effect on the daytime LST but a significant warming effect on nighttime LST (Fig. 6(b), Fig. 7(b)). This is consistent with the previous studies of Xia et al. (2016) and Zhou et al. (2012) in Texas, USA. The differential impacts are mainly caused by the large diurnal variation in atmospheric stability (Baidya et al., 2010). Wind turbines intensify the turbulent mixing in the atmospheric boundary layer and increase the sensible heat exchange between air and land, thus affecting LST (Chang et al., 2016; Rajewski et al., 2013). In the daytime, the atmosphere is unstable, with strong turbulent mixing, while the nighttime atmosphere is stable, suppressing the turbulent mixing in the boundary layer. In the area of wind farms, wind turbines rotate to mix cool air from the surface with warm air from the atmosphere. As a result, the enhanced turbulent mixing by wind farms plays a more important role at night than in the daytime. The Inner Mongolia Plateau, characterized by its continental climate with significant diurnal temperature variations, demonstrates more pronounced discrepancies in wind farm impacts on daytime and nighttime LST. Also, about the differences in different seasons, some previous research has found that the differences in wind speed among seasons would also affect the warming effect (Zhou et al., 2013). The nighttime wind speeds of summer and autumn in the Inner Mongolia plateau may lead to higher optimal wind speed frequency, which drives the wind turbine to produce more turbulence, resulting in more mixing of cold and warm air. This may explain why wind farms have a more substantial warming effect on nighttime LST in summer and autumn (Fig. 7(d)).

Many studies have found that land cover type affects the effect of wind farms on LST (Qin et al., 2022). Our results showed that the warming effect of wind farms on daytime and nighttime LST in grassland was stronger than that of forest and cropland (Fig. 6(c), Fig. 7(c)). Harris et al. (2014) and Qin et al. (2022) also found a similar result. Because the vegetation cover of grassland is usually lower than that of forest and cropland, it leads to the increase of surface albedo, which further leads to more reflected energy in grassland (Fitch et al., 2013). Therefore, the sensible heat flux of grassland is higher than that of forest and cropland in arid and semi-arid regions (Doran et al., 1995). The wind turbine leads to the exchange of sensible heat flux and upper cold air layer, leading to a stronger grassland warming effect (Kirk-Davidoff and Keith, 2008).

The impacts of wind farms on vegetation NPP are obvious (Tang et al., 2017).

Our study found that wind farms had an inhibitory effect on NPP under all land cover types (Fig. 8). This is consistent with Qin et al. (2022), which found wind farms weakened NPP in the USA. Removing vegetation for the construction of wind farms is one of the reasons for the reduction in NPP. Grasses, crops and trees are cleared to create wind turbine bases and roads for transporting materials (Turney and Fthenakis, 2011). So inevitably, this caused a drop in NPP. Additionally, soil moisture plays a crucial role in vegetation growth in arid and semi-arid regions (L. Liu et al., 2022). The warming effect of wind farms reduces soil moisture and leads to a decline in NPP (Tang et al., 2017). Meanwhile, the increase in nighttime LST would enhance vegetation respiration and further decrease NPP (Armstrong et al., 2014). Our study also found that the reduction of wind farms on NPP in forests is stronger than that in grassland (Fig. 8(c)). This may be because forest productivity per unit area is much higher than that of grassland. Further, grassland species tend to be more drought tolerant than forest species and thus have less productivity reduction (Brodrick et al., 2019).

In recent years, China has increasingly emphasized the strategic planning of wind farm construction. The development of wind farm should take technical, economic, environmental and social aspects into account (Dhunny et al., 2019; Kati et al., 2021). In this study, we focus on the impacts of wind farms on LST and NPP. It is acknowledged that wind farms also have additional direct impacts and potential effects. For instance, the construction of wind farms may lead to direct impacts such as changes in land cover, subsequently causing land degradation (Aksoy et al., 2023), habitat loss (Zimmerling et al., 2013), and fragmentation (Diffendorfer et al., 2019), thereby posing potential threats to biodiversity and raising other ecological concerns (Jones et al., 2015). Moreover, wind farms also bring challenges to culture and society (Bell et al., 2005; Jami and Walsh, 2017). We believe the potential impact of wind farms is a crucial direction for future research.

5. Conclusions

This study, for the first time, explored the landscape patterns changes of wind farms and their impacts on LST and NPP in the Inner Mongolia Plateau from 1990 to 2020. It is found that wind farms show a rapid growth trend, with 80.3% of wind farms constructed on grasslands, forming three aggregation areas in the central part. Wind farms generally have a warming effect on the nighttime LST with an average temperature increase of 0.23 °C, but only slightly affect daytime LST. At the same time, wind farms decreased NPP, with an average value of 12.37 GC/m^2. Compared to extensive wind farm research in Europe and North America, our study specifically focuses on the ecoclimatic impacts in Asia, providing in-depth insights into wind farm development in the Inner Mongolia Plateau and similar regions. Based on our findings, we recommend considering the potential impacts on local vegetation and climate when selecting sites for wind farm construction, especially in ecologically sensitive areas. This study hopes to provide a scientific reference for wind farm construction in the Inner Mongolia Plateau and globally.

References

Aksoy, T., Cetin, M., Cabuk, S.N., Senyel Kurkcuoglu, M.A., Bilge Ozturk, G., Cabuk, A., 2023. Impacts of wind turbines on vegetation and soil cover: a case study of Urla, Cesme, and Karaburun Peninsulas, Turkey. Clean Technol. Environ. Policy 25(1), 51-68.

Armstrong, A., Waldron, S., Whitaker, J., Ostle, N.J., 2014. Wind farm and solar park effects on plant–soil carbon cycling: uncertain impacts of changes in ground-level microclimate. Glob. Chang. Biol. 20(6), 1699-1706.

Avila, S., 2018. Environmental justice and the expanding geography of wind power conflicts. Sustain. Sci. 13(3), 599-616.

Ayodele, T.R., Ogunjuyigbe, A., Odigie, O., Munda, J.L., 2018. A multi-criteria GIS based model for wind farm site selection using interval type-2 fuzzy analytic hierarchy process: the case study of Nigeria. Appl. Energy 228, 1853-1869.

Baidya Roy, S., Traiteur, J.J., 2010. Impacts of wind farms on surface air temperatures. Proc. Natl. Acad. Sci. U.S.A. 107(42), 17899-17904.

Bell, D., Gray, T., Haggett, C., 2005. The ‘social gap’ in wind farm siting decisions: explanations and policy responses. Environ. Polit. 14(4), 460-477.

Bergström, L., Sundqvist, F., Bergström, U., 2013. Effects of an offshore wind farm on temporal and spatial patterns in the demersal fish community. Mar. Ecol. Prog. Ser. 485, 199-210.

Bonnier, A., Finné, M., Weiberg, E., 2019. Examining land-use through GIS-based kernel density estimation: a re-evaluation of legacy data from the berbati-limnes survey. J. Field Archaeol. 44(2), 70-83.

Brodrick, P., Anderegg, L., Asner, G., 2019. Forest drought resistance at large geographic scales. Geophys. Res. Lett. 46(5), 2752-2760.

Bureau, I.M.A.R.S., 2022. Statistical bulletin of Inner Mongolia Autonomous region’s national economic and social development in 2021. https://www.nmg.gov.cn/. (accessed 6 December 2022).

C2ES, 2020. Renewable Energy. https://www.c2es.org/content/renewable-energy/, Technology Solutions.

Chang, R., Zhu, R., Guo, P., 2016. A case study of land-surface-temperature impact from large-scale deployment of wind farms in China from Guazhou. Remote Sens. 8(10), 790.

Council, G.W.E., 2022. Global Wind Report 2022. https://gwec.net/global-wind-report-2022/. (accessed 7 December 2022).

Dai, J., Yang, X., Wen, L., 2018. Development of wind power industry in China: a comprehensive assessment. Renew. Sust. Energ. Rev. 97, 156-164.

Dai, Y., Xue, L., 2015. China’s policy initiatives for the development of wind energy technology. Clim. Policy 15(1), 30-57.

Deng, Y., Yu, Z., Liu, S., 2011. A review on scale and siting of wind farms in China. Wind Energy 14(3), 463-470.

Dhunny, A.Z., Allam, Z., Lobine, D., Lollchund, M.R., 2019. Sustainable renewable energy planning and wind farming optimization from a biodiversity perspective. Energy 185, 1282-1297.

Diffendorfer, J.E., Dorning, M.A., Keen, J.R., Kramer, L.A., Taylor, R.V., 2019. Geographic context affects the landscape change and fragmentation caused by wind energy facilities. PeerJ 7, e7129.

Dong, Y., Wang, J., Jiang, H., Shi, X., 2013. Intelligent optimized wind resource assessment and wind turbines selection in Huitengxile of Inner Mongolia, China. Appl. Energy 109, 239-253.

Doran, J., Shaw, W., Hubbe, J., 1995. Boundary layer characteristics over areas of inhomogeneous surface fluxes. J. Appl. Meteorol. Climatol. 34(2), 559-571.

Drewitt, A.L., Langston, R.H., 2006. Assessing the impacts of wind farms on birds. Ibis 148, 29-42.

Fagúndez, J., 2009. Effects of wind farm construction and operation on mire and wet heath vegetation in the Monte Maior SCI, north-west Spain. Mires and Peat 4.

Fitch, A.C., Olson, J.B., Lundquist, J.K., 2013. Parameterization of wind farms in climate models. J. Clim. 26(17), 6439-6458.

Fox, A., Desholm, M., Kahlert, J., Christensen, T.K., Krag Petersen, I., 2006. Information needs to support environmental impact assessment of the effects of European marine offshore wind farms on birds. Ibis 148, 129-144.

Guo, X., Zhang, X., Du, S., Li, C., Siu, Y.L., Rong, Y., Yang, H., 2020. The impact of onshore wind power projects on ecological corridors and landscape connectivity in Shanxi, China. J. Clean. Prod. 254, 120075.

Haines, A., Smith, K.R., Anderson, D., Epstein, P.R., McMichael, A.J., Roberts, I., Wilkinson, P., Woodcock, J., Woods, J., 2007. Policies for accelerating access to clean energy, improving health, advancing development, and mitigating climate change. Lancet 370(9594), 1264-1281.

Harris, R.A., Zhou, L., Xia, G., 2014. Satellite observations of wind farm impacts on nocturnal land surface temperature in Iowa. Remote Sens. 6(12), 12234-12246.

Howland, M.F., Lele, S.K., Dabiri, J.O., 2019. Wind farm power optimization through wake steering. Proc. Natl. Acad. Sci. U.S.A. 116(29), 14495-14500.

Hurtado, J.P., Fernández, J., Parrondo, J.L., Blanco, E., 2004. Spanish method of visual impact evaluation in wind farms. Renew. Sust. Energ. Rev. 8(5), 483-491.

Institute of Geographic Sciences and Natural Resources Research, Chinese Academy of Sciences, 2007. Inner Mongolian Plateau. http://www.igsnrr.cas.cn/cbkx/kpyd/zgdl/cndm/202009/t20200910_5692371.html. (accessed 6 December 2022).

Jami, A.A., Walsh, P.R., 2017. From consultation to collaboration: A participatory framework for positive community engagement with wind energy projects in Ontario, Energy Res. Soc. Sci. 27, 14-24.

Jones, N.F., Pejchar, L., Kiesecker, J.M., 2015. The energy footprint: how oil, natural gas, and wind energy affect land for biodiversity and the flow of ecosystem services. BioScience 65(3), 290-301.

Kati, V., Kassara, C., Vrontisi, Z., Moustakas, A., 2021. The biodiversity-wind energy-land use nexus in a global biodiversity hotspot. Sci. Total Environ. 768, 144471.

Keith, D.W., DeCarolis, J.F., Denkenberger, D.C., Lenschow, D.H., Malyshev, S.L., Pacala, S., Rasch, P.J., 2004. The influence of large-scale wind power on global climate. Proc. Natl. Acad. Sci. U.S.A. 101(46), 16115-16120.

Kemp, L., Xu, C., Depledge, J., Ebi, K.L., Gibbins, G., Kohler, T.A., Rockström, J., Scheffer, M., Schellnhuber, H.J., Steffen, W., 2022. Climate Endgame: Exploring catastrophic climate change scenarios. Proc. Natl. Acad. Sci. U.S.A. 119(34), e2108146119.

Kirk-Davidoff, D.B., Keith, D.W., 2008. On the climate impact of surface roughness anomalies. J. Atmos. Sci. 65(7), 2215-2234.

Lashof, D.A., Ahuja, D.R., 1990. Relative contributions of greenhouse gas emissions to global warming. Nature 344(6266), 529-531.

Leung, D.Y., Yang, Y., 2012. Wind energy development and its environmental impact: a review. Renew. Sust. Energ. Rev. 16(1), 1031-1039.

Li, Y., Kalnay, E., Motesharrei, S., Rivas, J., Kucharski, F., Kirk-Davidoff, D., Bach, E., Zeng, N., 2018. Climate model shows large-scale wind and solar farms in the Sahara increase rain and vegetation. Science 361(6406), 1019-1022.

Liu, L., Xu, X., Wu, J., Jarvie, S., Li, F., Han, P., Zhang, Q., 2022. Comprehensive evaluation and scenario simulation of carrying capacity of water resources in Mu Us sandy land, China. Water Supply 22(9), 7256-7271.

Liu, P., Liu, L., Xu, X., Zhao, Y., Niu, J., Zhang, Q., 2021. Carbon footprint and carbon emission intensity of grassland wind farms in Inner Mongolia. J. Clean. Prod. 313, 127878.

Liu, T., Chen, Z., Xu, J., 2022. Empirical evidence based effectiveness assessment of policy regimes for wind in China. Renew. Sust. Energ. Rev. 164, 112535.

Liu, Y., Dang, B., Xu, Y., Weng, F., 2021. An observational study on the local climate effect of the Shangyi wind farm in Hebei Province. Adv. Atmos. Sci. 38(11), 1905-1919.

Luo, L., Zhuang, Y., Duan, Q., Dong, L., Yu, Y., Liu, Y., Chen, K., Gao, X., 2021. Local climatic and environmental effects of an onshore wind farm in North China. Agric. For. Meteorol. 308, 108607.

Moradi, S., Yousefi, H., Noorollahi, Y., Rosso, D., 2020. Multi-criteria decision support system for wind farm site selection and sensitivity analysis: case study of Alborz Province, Iran. Energy Strategy Rev. 29, 100478.

Moravec, D., Bartak, V., Pus, V., Wild, J., 2018. Wind turbine impact on near-ground air temperature. Renew. Energ. 123, 627-633.

Qin, Y., Li, Y., Xu, R., Hou, C., Armstrong, A., Bach, E., Wang, Y., Fu, B., 2022. Impacts of 319 wind farms on surface temperature and vegetation in the United States. Environ. Res. Lett. 17(2), 024026.

Rajewski, D.A., Takle, E.S., Lundquist, J.K., Oncley, S., Prueger, J.H., Horst, T.W., Rhodes, M.E., Pfeiffer, R., Hatfield, J.L., Spoth, K.K., 2013. Crop wind energy experiment (CWEX): observations of surface-layer, boundary layer, and mesoscale interactions with a wind farm. Bull. Am. Meteorol. Soc. 94, 655-672.

Saidur, R., Rahim, N.A., Islam, M.R., Solangi, K.H., 2011. Environmental impact of wind energy. Renew. Sust. Energ. Rev. 15(5), 2423-2430.

Sawant, M., Thakare, S., Rao, A.P., Feijóo-Lorenzo, A.E., Bokde, N.D., 2021. A review on state-of-the-art reviews in wind-turbine-and wind-farm-related topics. Energies 14(8), 2041.

Schumaker, N.H., 1996. Using landscape indices to predict habitat connectivity. Ecology 77, 1210-1225.

Sibille, A.d.C.T., Cloquell-Ballester, V.-A., Cloquell-Ballester, V.-A., Darton, R., 2009. Development and validation of a multicriteria indicator for the assessment of objective aesthetic impact of wind farms. Renew. Sust. Energ. Rev. 13(1), 40-66.

Slawsky, L.M., Zhou, L., Roy, S.B., Xia, G., Vuille, M., Harris, R.A., 2015. Observed thermal impacts of wind farms over Northern Illinois. Sensors 15(7), 14981-15005.

Steffen, W., Rockström, J., Richardson, K., Lenton, T.M., Folke, C., Liverman, D., Summerhayes, C.P., Barnosky, A.D., Cornell, S.E., Crucifix, M., 2018. Trajectories of the earth system in the Anthropocene. Proc. Natl. Acad. Sci. U.S.A. 115(33), 8252-8259.

Su, N., Jarvie, S., Yan, Y., Gong, X., Li, F., Han, P., Zhang, Q., 2022. Landscape context determines soil fungal diversity in a fragmented habitat. Catena 213, 106163.

Tang, B., Wu, D., Zhao, X., Zhou, T., Zhao, W., Wei, H., 2017. The observed impacts of wind farms on local vegetation growth in northern China. Remote Sens. 9(4), 332.

Turney, D., Fthenakis, V., 2011. Environmental impacts from the installation and operation of large-scale solar power plants. Renew. Sust. Energ. Rev. 15(6), 3261-3270.

Van der Horst, D., Toke, D., 2010. Exploring the landscape of wind farm developments; local area characteristics and planning process outcomes in rural England. Land Use Policy 27(2), 214-221.

Van Haaren, R., Fthenakis, V., 2011. GIS-based wind farm site selection using spatial multi-criteria analysis (SMCA): evaluating the case for New York State. Renew. Sust. Energ. Rev. 15(7), 3332-3340.

Wu, J., Wang, J., Chi, D., 2013. Wind energy potential assessment for the site of Inner Mongolia in China. Renew. Sust. Energ. Rev. 21, 215-228.

Xia, C., Song, Z., 2009. Wind energy in China: Current scenario and future perspectives. Renew. Sust. Energ. Rev. 13(8), 1966-1974.

Xia, G., Zhou, L., 2017. Detecting wind farm impacts on local vegetation growth in Texas and Illinois using MODIS vegetation greenness measurements. Remote Sens. 9(7), 698.

Xia, G., Zhou, L., Freedman, J.M., Roy, S.B., Harris, R.A., Cervarich, M.C., 2016. A case study of effects of atmospheric boundary layer turbulence, wind speed, and stability on wind farm induced temperature changes using observations from a field campaign. Clim. Dyn. 46(7-8), 2179-2196.

Xu, K., He, L., Hu, H., Liu, S., Du, Y., Wang, Z., Li, Y., Li, L., Khan, A., Wang, G., 2019. Positive ecological effects of wind farms on vegetation in China's Gobi desert. Sci. Rep. 9(1), 1-11.

Yuan, J., Bian, Z., Yan, Q., Gu, Z., Yu, H., 2020. An approach to the temporal and spatial characteristics of vegetation in the growing season in Western China. Remote Sens. 12(6), 945.

Zeng, B., Zeng, M., Xue, S., Cheng, M., Wang, Y., Feng, J., 2014. Overall review of wind power development in Inner Mongolia: status quo, barriers and solutions. Renew. Sust. Energ. Rev. 29, 614-624.

Zhang, Q., Buyantuev, A., Fang, X., Han, P., Li, A., Li, F.Y., Liang, C., Liu, Q., Ma, Q., Niu, J., 2020. Ecology and sustainability of the Inner Mongolian Grassland: Looking back and moving forward. Landscape Ecol. 35, 2413-2432.

Zhang, S., Wei, J., Chen, X., Zhao, Y., 2020. China in global wind power development: Role, status and impact. Renew. Sust. Energ. Rev. 127, 109881.

Zhang, X., Xu, L., Chen, Y., Liu, T., 2020. Emergy-based ecological footprint analysis of a wind farm in China. Ecol. Indic. 111, 106018.

Zhou, L., Tian, Y., Roy, S.B., Dai, Y., Chen, H., 2013. Diurnal and seasonal variations of wind farm impacts on land surface temperature over western Texas. Clim. Dyn. 41, 307-326.

Zhou, L., Tian, Y., Roy, S.B., Thorncroft, C., Bosart, L.F., Hu, Y., 2012. Impacts of wind farms on land surface temperature. Nat. Clim. Chang. 2(7), 539-543.

Zimmerling, J., Pomeroy, A., d'Entremont, M., Francis, C., 2013. Canadian estimate of bird mortality due to collisions and direct habitat loss associated with wind turbine developments. Avian Conserv. Ecol. 8(2), 1-13.

Declaration of Competing Interest

No conflict of interest exits in the submission of this manuscript, and manuscript is approved by all authors for publication. I would like to declare on behalf of my co-authors that the work described was original research that has not been published previously, and not under consideration for publication elsewhere, in whole or in part. All the authors listed have approved the manuscript that is enclosed.